Appendix A

The RAMONA/POLCA Model

A.1 Neutron Kinetics and Power Generation

The most rigorous description of the neutron flux behavior is given by the Boltzmann transport equation. A numerical solution of this fully three dimensional problem is prohibitively expensive in computer time and memory. Therefore the following simplifications are standard in 3D numerical reactor models and proven to be acceptable.

- The energy dependence is characterized by two energy groups.

  The border between thermal and fast neutrons is set at 1 eV such that neutrons in the thermal group do not scatter up into the fast group.

- Using Fick's law, the transport equation is simplified into a diffusion equation.

  The solution of the core neutronics requires the definition of average cross sections. The complex geometry of a fuel assembly cannot be modeled precisely with the Diffusion equation and the coarse mesh used to calculate reactor wide data. A homogenization is carried out by first obtaining a fine-mesh (2-D), multi group transport code theory solution for the fuel cell using zero current boundary conditions. Then, flux weighting of the multi group cross sections is performed to obtain the equivalent two-group parameters for the homogenized fuel cell. For example, the node averaged total cross section for energy group g is

$$\overline{\Sigma_{t,g}} = \frac{\int\limits_{fuelcell} dV \int\limits_{\Delta E_g} dE \cdot \Sigma_t(r,E)\,\varphi(r,E)}{\int\limits_{fuelcell} dV \int\limits_{\Delta E_g} dE \cdot \varphi(r,E)} \tag{A.1}$$

  where $\varphi(r,E)$ is the fine mesh, multi-group flux solution for the fuel cell obtained from detailed auxiliary calculations performed e.g. with the lattice physics code PHOENIX [2]. ΔE_g is the energy width of the group g. The first integration is the homogenization procedure and the second integration is the energy averaging procedure known as

group collapsing. All lattice code calculations are conducted in this work by the steady state core simulators PRESTO or POLCA. MATSTAB reads the required data from the master files generated by these steady state codes (see Figure 2.2 on page 19).

- The time dependence of the delayed neutrons is characterized by 6 delayed groups.

A.1.1 Governing Equations for Neutron Kinetics

The general diffusion theory equation is derived from the equation of continuity which states, that the rate of change in number of neutrons is equal to the rate of production minus the rate of absorption minus the rate of leakage of neutrons within a volume of interest. See any reactor physics textbook for an in-depth explanation, e.g. [48].

$$\frac{1}{V}\frac{\partial \varphi}{\partial \tau} = source - \Sigma_{absorption}\varphi - \mathrm{div}\mathbf{J} \tag{A.2}$$

The neutron leakage term is obtained by applying Fick's Law.

$$\mathbf{J} = -D\nabla\varphi \tag{A.3}$$

Inserting **J** in the equation of continuity, assuming that D is not a function of position gives

$$\frac{1}{V}\frac{\partial \varphi}{\partial \tau} = D\nabla^2\varphi - \Sigma_{absorption}\varphi + source \tag{A.4}$$

The two-group equations with more detailed absorption and production terms are:

Diffusion equation for the fast neutron flux

$$\frac{1}{V_1}\frac{\partial \varphi_1}{\partial \tau} = D_1\nabla^2\varphi_1 - (\Sigma_{a1} + \Sigma_r)\varphi_1 + (1-\beta)\left(\nu_1\Sigma_{f1}\varphi_1 + \nu_2\Sigma_{f2}\varphi_2\right) + \sum_d \lambda_d C_d \tag{A.5}$$

(A.6)

Diffusion equation for the thermal neutron flux

$$\frac{1}{V_2}\frac{\partial \varphi_2}{\partial \tau} = D_2\nabla^2\varphi_2 - \Sigma_{a2}\varphi_2 + \Sigma_r\varphi_1 \tag{A.7}$$

Precursors of delayed neutrons for group d

$$\frac{\partial C_d}{\partial \tau} = \beta_d\left(\nu_1\Sigma_{f1}\varphi_1 + \nu_2\Sigma_{f2}\varphi_2\right) - \lambda_d C_d \tag{A.8}$$

A.1.2 Boundary Conditions

The core of a BWR is surrounded by the coolant which acts as a reflector for both fast and thermal neutrons. A reflector can significantly affect the characteristics of the neutron population within the core. It is therefore important to represent correctly the effects produced by a reflector. Fick's Law is not valid in the immediate vicinity of the surface of the core, so another approach has to be found. It would be possible to simply include the reflector as a part of the overall reactor. However, this way is computationally costly since fine meshes are required to represent the reflector in a finite-difference approximation. MATSTAB uses another common approach which overcomes this problem by excluding the reflector but, instead, applying appropriate boundary conditions at the core-reflector interfaces. The most general approach for the two-group approximation is to use a matrix albedo **a** defined at the surface of the core. The following equations originate from the model used in POLCA and are described in detail in [52].

$$\mathbf{J}^{return} = \mathbf{a} \cdot \mathbf{J}^{out} \tag{A.9}$$

$$\mathbf{a} = \begin{bmatrix} a_{11} & 0 \\ a_{21} & a_{22} \end{bmatrix}, \quad \mathbf{J} = \begin{bmatrix} J_1 \\ J_2 \end{bmatrix} \tag{A.10}$$

The values of $\mathbf{a_{ij}}$ are taken from the master file of the steady state code.

A.1.3 Node Integrated Balance Equations

The nodalization of the core leads to node averaged quantities, denoted with a bar.

$$\bar{\varphi}_1 = \frac{1}{h_x h_y h_z} \int_{\substack{volume \\ of node}} \varphi_1 dr \tag{A.11}$$

and

$$\begin{aligned} \frac{1}{V_1} \frac{\partial \bar{\varphi}_{1n}}{\partial \tau} = \frac{1}{h_x h_y h_z} \int_{\substack{volume \\ of node}} \nabla D_1 \nabla \varphi_1 dr - (\Sigma_{a1} + \Sigma_r) \bar{\varphi}_{1n} \\ + (1-\beta)\left(\nu_1 \Sigma_{f1} \bar{\varphi}_{1n} + \nu_2 \Sigma_{f2} \bar{\varphi}_{2n}\right) + \sum_d \lambda_d \bar{C}_d \end{aligned} \tag{A.12}$$

for the fast neutron flux. By means of the divergence theorem, we can rewrite the volume integral as a surface integral

$$\frac{1}{h_x h_y h_z} \int_{\substack{volume \\ of node}} \nabla D_1 \nabla \varphi_1 dr = \frac{1}{h_x h_y h_z} \int_{\substack{surface \\ of node}} D_1 \nabla \varphi_1 dA = -\sum_{m=1}^{6} \frac{1}{h_{nm}} \mathbf{J}_{1,nm} \tag{A.13}$$

Where n is the number of the node and m is one of its neighbors. The node integrated balance equations for the node n therefore look as follows.

$$\frac{1}{V_1}\frac{d\bar{\varphi}_{1n}}{d\tau} = -\sum_{m=1}^{6}\frac{1}{h_{nm}}\mathbf{J}_{1,nm} - (\Sigma_{a1}+\Sigma_r)\bar{\varphi}_{1n} + (1-\beta)\left(\nu_1\Sigma_{f1}\bar{\varphi}_{1n} + \nu_2\Sigma_{f2}\bar{\varphi}_{2n}\right) + \sum_d \lambda_d \bar{C}_d \tag{A.14}$$

$$\frac{1}{V_2}\frac{d\bar{\varphi}_{2n}}{d\tau} = -\sum_{m=1}^{6}\frac{1}{h_{nm}}\mathbf{J}_{2,nm} - \Sigma_{a2}\bar{\varphi}_{2n} + \Sigma_r\bar{\varphi}_{1n} \tag{A.15}$$

$$\frac{d\bar{C}_{dn}}{d\tau} = \beta_d\left(\nu_1\Sigma_{f1}\bar{\varphi}_{1n} + \nu_2\Sigma_{f2}\bar{\varphi}_{2n}\right) - \lambda_d\bar{C}_{dn} \tag{A.16}$$

The expression relating the node interface net currents to the average fluxes of the adjacent nodes is

$$\frac{1}{h_{nm}}\mathbf{J}_{g,nm} = \mathbf{X}_{g,nm}\bar{\varphi}_{1,n} - \mathbf{Y}_{g,nm}\bar{\varphi}_{1,m} \tag{A.17}$$

where h_{nm} is the extension of node n in the nm direction. The complete derivation is found in [52],[48]. The coupling coefficients are given by

$$\mathbf{X}_{1,nm} = \frac{R_{nm}}{h_x^2}\sqrt{\tilde{D}_{1n}}\,\sqrt{\tilde{D}_{1m}}\,q_n\,s_n \tag{A.18}$$

$$\mathbf{Y}_{1,nm} = \frac{R_{nm}}{h_x^2}\sqrt{\tilde{D}_{1n}}\,\sqrt{\tilde{D}_{1m}}\,q_m\,s_m \tag{A.19}$$

$$\mathbf{X}_{2,nm} = \frac{R_{nm}}{h_x^2}\sqrt{\tilde{D}_{2n}}\,\sqrt{\tilde{D}_{2m}}\,q_n\,s_n\,r_{\infty n} \tag{A.20}$$

$$\mathbf{Y}_{2,nm} = \frac{R_{nm}}{h_x^2}\sqrt{\tilde{D}_{2n}}\,\sqrt{\tilde{D}_{2m}}\,q_m\,s_m\,r_{\infty m} \tag{A.21}$$

$$\mathbf{X}_{1,nr} = \frac{2}{h_{nr}^2}\frac{\tilde{D}_{1n}\tilde{D}_{1r}}{\tilde{D}_{1n}+\tilde{D}_{1r}}q_n s_n \tag{A.22}$$

$$\mathbf{Y}_{1,nr} = 0 \tag{A.23}$$

$$\mathbf{X}_{2,nr} = \frac{2}{h_{nr}^2}\left[\frac{\tilde{D}_{2n}\tilde{D}_{2r}}{\tilde{D}_{2n}+\tilde{D}_{2r}} - \frac{\frac{C_{21}}{r_{\infty n}}}{\left(\frac{1}{\tilde{D}_{1n}}+\frac{1}{\tilde{D}_{1r}}\right)\left(\frac{1}{\tilde{D}_{2n}}+\frac{1}{\tilde{D}_{2r}}\right)}\right] q_n\,s_n\,r_{\infty n} \tag{A.24}$$

$$\mathbf{Y}_{2,nr} = 0 \tag{A.25}$$

where

Node size ratios

$R_{nm} = 1$, m points in x,y-direction

$R_{nm} = \frac{h_x^2}{h_z^2}$, m points in z-direction

$R_{nr} = 0$, m points to reflector

$r_\infty = \frac{\Sigma_r}{\Sigma_{a2}}$

Infinite multiplication factor

$$k_\infty = \tilde{\beta}\frac{\nu_1\Sigma_{f1}+r_\infty\nu_2\Sigma_{f2}}{\Sigma_{a1}}$$

$$\tilde{\beta} = 1-\beta+\sum_d \frac{\beta_d\lambda_d}{\lambda+\lambda_d}$$

$$\Lambda = \frac{D_1}{\Sigma_{a1}}$$

Thermal diffusion length

$$L^2 = \frac{D_2}{\Sigma_{a2}}$$

$$\chi = \frac{L^2}{\Lambda}$$

$$l^2 = \frac{h_x^2}{2+\frac{h_x^2}{h_z^2}}$$

$$b_1^2 = \frac{1}{4}l^2\frac{k_\infty-1}{L^2+\Lambda}$$

$$b_2^2 = \frac{3}{4}l^2\frac{1+\chi}{L^2}$$

$$t_1 = 1-\frac{1}{3}b_1^2$$

$$s_n = 1+\frac{2}{3}b_1^2$$

$$t_2 = b_2-c_p(b_2-t_1)$$

$$\tilde{D}_g = D_g t_g$$

$$\tilde{D}_{1r} = \frac{h_{nr}}{4}\frac{1-a_{11}}{1+a_{11}}$$

$$\tilde{D}_{2r} = \frac{h_{nr}}{4}\frac{1-a_{22}}{1+a_{22}}$$

$$C_{21} = \frac{8}{h_{nr}}\frac{a21}{(1-a_{11})(1-a_{22})}$$

$$r_n = \frac{\varphi_2}{\varphi_1}$$

$$q_n = 1+\frac{\chi}{1+\chi}\left(\frac{r}{r_\infty}-1\right)$$

A.1.4 Prompt Jump Approximation

The time derivative of the fast and the thermal flux are both set to zero, which means that the left hand side of A.14 and A.15 are set to zero.

$$\begin{aligned}0 = &-\left[\sum_{m=1}^{6}\mathbf{X}_{1,nm}+\Sigma_{a1}+\Sigma_r\right]\bar{\varphi}_{1n}+\sum_{m=1}^{6}\mathbf{Y}_{1,nm}\bar{\varphi}_{1m}\\ &+(1-\beta)(\nu_1\Sigma_{f1}\bar{\varphi}_{1n}+\nu_2\Sigma_{f2}\bar{\varphi}_{2n})-\sum_d\lambda_d\bar{C}_{dn}\end{aligned} \tag{A.26}$$

$$0 = -\left[\sum_{m=1}^{6}\mathbf{X}_{2,nm}-\Sigma_r\right]\bar{\varphi}_{1n}+\sum_{m=1}^{6}\mathbf{Y}_{2,nm}\bar{\varphi}_{1m}-\Sigma_{a2}\bar{\varphi}_{2n} \tag{A.27}$$

The prompt jump approximation is valid, if the life time of a neutron is much smaller than the studied phenomena. Physically it is an immediate adaption of the neutron flux to perturbations.

The life time of some precursors is much closer to the time a density wave needs to pass the reactor than the neutron life time and, therefore, significant. The time derivative of the precursors may not be set to zero. Nevertheless it is possible to simplify equation A.16 without much loss in accuracy.

Equation 2.25 describes the time dependence of a state variable. For the variable $\bar{C}_d(\tau)$ it reads as follows.

$$\bar{C}_{dn}(\tau) = \bar{c}_{dn} e^{\lambda\tau} \quad , d = 1, \ldots, 6 \tag{A.28}$$

Where $\bar{c}_{dn}$ is a scalar and not time dependent. Equation A.16 may now be written as follows.

$$\frac{d\bar{c}_{dn} e^{\lambda\tau}}{d\tau} = \beta_d (\nu_1 \Sigma_{f1} \bar{\varphi}_{1n} + \nu_2 \Sigma_{f2} \bar{\varphi}_{2n}) - \lambda_d \bar{C}_{dn} \tag{A.29}$$

It is now possible to carry out the derivation with respect to time. This transforms the differential equation into a algebraic equation.

$$\lambda \bar{C}_{dn} = \beta_d (\nu_1 \Sigma_{f1} \bar{\varphi}_{1n} + \nu_2 \Sigma_{f2} \bar{\varphi}_{2n}) - \lambda_d \bar{C}_{dn} \tag{A.30}$$

$\bar{C}_{dn}$ is depending on λ which actually is unknown. Therefore the starting guess of λ is used to calculate $\bar{C}_{dn}$. This simplification is good enough, as long as the starting guess for λ is reasonable. The draw back is however, that λ is complex and therefore the matrix $\mathbf{A}$ becomes complex too. It remains to mention that this equation is used for the POLCA model as well as for the RAMONA model.

Inserting A.31 into A.26 yields

$$\bar{C}_{dn} = \frac{\beta_d}{\lambda - \lambda_d} (\nu_1 \Sigma_{f1} \bar{\varphi}_{1n} + \nu_2 \Sigma_{f2} \bar{\varphi}_{2n}) \tag{A.31}$$

Inserting A.31 into A.26 yields

$$\begin{aligned} 0 = &- \left[\sum_{m=1}^{6} \mathbf{X}_{1,nm} + \Sigma_{a1} + \Sigma_r \right] \bar{\varphi}_{1n} + \sum_{m=1}^{6} \mathbf{Y}_{1,nm} \bar{\varphi}_{1m} \\ &+ \tilde{\beta} (\nu_1 \Sigma_{f1} \bar{\varphi}_{1n} + \nu_2 \Sigma_{f2} \bar{\varphi}_{2n}) \end{aligned} \tag{A.32}$$

where

$$\tilde{\beta} = 1 - \beta + \sum_d \frac{\beta_d \lambda_d}{\lambda + \lambda_d} \tag{A.33}$$

Solving A.27 for $\bar{\varphi}_{2n}$ yields

$$\bar{\varphi}_{2n} = \frac{\left[\Sigma_r - \sum_{m=1}^{6} \mathbf{X}_{2,nm}\right]}{\Sigma_{a2}} \bar{\varphi}_{1n} + \frac{\sum_{m=1}^{6} \mathbf{Y}_{2,nm}}{\Sigma_{a2}} \bar{\varphi}_{1m}. \tag{A.34}$$

Inserting the solution into A.32 leads to

$$\begin{aligned} 0 = &- \left[\sum_{m=1}^{6} \mathbf{X}_{1,nm} + \Sigma_{a1} + \Sigma_r - \tilde{\beta}\nu_1\Sigma_{f1} - \tilde{\beta}\nu_2\Sigma_{f2} \frac{\left[\Sigma_r - \sum_{m=1}^{6} \mathbf{X}_{2,nm}\right]}{\Sigma_{a2}} \right] \bar{\varphi}_{1n} \\ &+ \left[\sum_{m=1}^{6} \mathbf{Y}_{1,nm} + \tilde{\beta}\nu_2\Sigma_{f2} \frac{\sum_{m=1}^{6} \mathbf{Y}_{2,nm}}{\Sigma_{a2}} \right] \bar{\varphi}_{1m} \end{aligned} \tag{A.35}$$

and

$$\bar{\varphi}_{1n} = \frac{\sum_{m=1}^{6} \left(\mathbf{Y}_{1,nm} + \tilde{\beta} \frac{\nu_2\Sigma_{f2}}{\Sigma_{a2}} \mathbf{Y}_{2,nm} \right) \bar{\varphi}_{1m}}{\sum_{m=1}^{6} (\mathbf{X}_{1,nm} + \tilde{\beta} \frac{\nu_2\Sigma_{f2}}{\Sigma_{a2}} \mathbf{X}_{2,nm}) - \Sigma_{a1}(k_\infty - 1)} \equiv \sum_{m=1}^{6} \mathbf{A}_{nm} \bar{\varphi}_{1m} \tag{A.36}$$

A.1.5 Linearization

Linearizing the neutronics means to linearize A.36.

$$\begin{aligned} \Delta\bar{\varphi}_{1n} &= \frac{\partial\bar{\varphi}_{1n}}{\partial\bar{\varphi}_{1m}} \Delta\bar{\varphi}_{1m} + \frac{\partial\bar{\varphi}_{1n}}{\partial\alpha} \Delta\alpha + \frac{\partial\bar{\varphi}_{1n}}{\partial t} \Delta t \\ &= \sum_{m=1}^{6} \mathbf{A}_{nm} \Delta\bar{\varphi}_{1m} + \sum_{m=1}^{6} \frac{[\mathbf{A}_{nm}(\alpha + \Delta\alpha) - \mathbf{A}_{nm}(\alpha)]\bar{\varphi}_{1m}}{\Delta\alpha} \Delta\alpha \\ &\quad + \sum_{m=1}^{6} \frac{[\mathbf{A}_{nm}(t + \Delta t) - \mathbf{A}_{nm}(t)]\bar{\varphi}_{1m}}{\Delta t} \Delta t \end{aligned} \tag{A.37}$$

To calculate A.37 one needs to know $D_1, D_2, \Sigma_{a1}, \Sigma_{a2}, \Sigma_r, \nu_1\Sigma_{f1}, \nu_2\Sigma_{f2}, \nu_1$ and ν_2 for $\alpha, \alpha + \Delta\alpha, t$ and for $t + \Delta t$. These values are calculated with the help of the tables generated for the steady state core simulator. The tables are stored in the master file, and therefore available without problems. Therefore the linearization with respect to the void and temperature dependence is done numerically.

A.1.6 Power Generation

MATSTAB takes into account the fact, that the fission energy is deposited as thermal energy both inside the fuel pellet where the fission takes place and outside the pellet due to neutron slowing down and gamma ray attenuation.

The total power generation rate in the fuel is

$$\bar{q}''' = K\,(1 - H\,(0, \infty))\,(\Sigma_{f1}\bar{\varphi}_{1n} + \Sigma_{f2}\bar{\varphi}_{2n}) \tag{A.38}$$

where $H(0,\infty) = 0.07$ and $K = 3.2 \cdot 10^{11}$ Joule/Fission.

The thermal flux in A.38 is eliminated with the help of A.34.

$$\begin{aligned} \bar{q}''' &= K(1-H(0,\infty)) \left(\left[\Sigma_{f1} + \frac{\Sigma_{f2}}{\Sigma_{a2}} \left(\Sigma_r - \sum_{m=1}^{6} \mathbf{X}_{2,nm} \right) \right] \bar{\varphi}_{1n} + \frac{\Sigma_{f2}}{\Sigma_{a2}} \sum_{m=1}^{6} \mathbf{Y}_{2,nm} \bar{\varphi}_{1m} \right) \\ &\equiv \mathbf{A}_{qn} \bar{\varphi}_{1n} + \mathbf{A}_{qm} \bar{\varphi}_{1m} \end{aligned} \tag{A.39}$$

A.1.7 Linearization

The linearization of A.39 reads as follows.

$$\begin{aligned} \Delta\bar{q}''' &= \frac{\partial \bar{q}'''}{\partial \bar{\varphi}_{1n}} \Delta\bar{\varphi}_{1n} + \frac{\partial \bar{q}'''}{\partial \bar{\varphi}_{1m}} \Delta\bar{\varphi}_{1m} + \frac{\partial \bar{q}'''}{\partial \alpha} \Delta\alpha + \frac{\partial \bar{q}'''}{\partial t} \Delta t \\ &\approx \mathbf{A}_{qn} \Delta\bar{\varphi}_{1n} + \mathbf{A}_{qm} \Delta\bar{\varphi}_{1m} \\ &\quad + \frac{\mathbf{A}_{qn}(\alpha+\delta\alpha) - \mathbf{A}_{qn}(\alpha)}{\delta\alpha} \bar{\varphi}_{1n} \Delta\alpha \\ &\quad + \frac{\mathbf{A}_{qm}(\alpha+\delta\alpha) - \mathbf{A}_{qm}(\alpha)}{\delta\alpha} \bar{\varphi}_{1m} \Delta\alpha \\ &\quad + \frac{\mathbf{A}_{qn}(t+\delta t) - \mathbf{A}_{qn}(t)}{\delta t} \bar{\varphi}_{1n} \Delta t \\ &\quad + \frac{\mathbf{A}_{qm}(t+\delta t) - \mathbf{A}_{qm}(t)}{\delta t} \bar{\varphi}_{1m} \Delta t \end{aligned} \tag{A.40}$$

A.2 Modeling of Thermal Conduction

Associated with each neutronic node is an average fuel pin for which the thermal energy source and heat conduction are calculated. The calculated average fuel temperature feeds back into the neutronics (Doppler effect) and the calculated heat flux from the cladding surface enters the hydraulics calculations.

A.2.1 Field Equation of Thermal Conduction

The thermal energy storage and conduction in the fuel pins, consisting of the fuel pellets, of the gas gap between pellet and cladding and of the fuel cladding is modeled with the following assumptions.

- Fuel and cladding are rigid, retaining their cylindrical geometries. Possible variations in time of the gas gap width can be taken into account by a temperature dependent gap conductance.
- The volumetric heat generation q'''_f is uniformly distributed over the fuel pellet cross section. Gamma heat generation in the gas gap and the cladding is ignored.
- Axial and azimuthal conduction is negligible
- The thermal properties like heat capacity, conductivity etc. can be represented with the correlations stated below.

The general form of the heat conduction equation

$$\rho c \frac{\partial t}{\partial \tau} = \nabla (k \nabla t) + q''' \tag{A.41}$$

is formulated for the fuel and for the cladding separately. After neglecting axial and azimuthal conduction the equation looks as follows.

Pellet:

$$(\rho c)_f \frac{\partial t_f}{\partial \tau} = \frac{1}{r} \frac{\partial}{\partial r} \left(r k_f \frac{\partial t_f}{\partial r} \right) + q'''_f \quad , 0 \leq r < R_f \quad , \tau > 0 \tag{A.42}$$

with the boundary conditions:

$$\begin{aligned} \left. \frac{\partial t_f}{\partial r} \right|_{r=0} &= 0 && \text{, for all } \tau \\ k_f \left. \frac{\partial t_f}{\partial r} \right|_{r=R_f} &= \frac{k_{gp}}{\delta} \left[t_c (R_{ci}) - t_f (R_f) \right] && \text{, for all } \tau \end{aligned} \tag{A.43}$$

Cladding:

$$(\rho c)_c \frac{\partial t_c}{\partial \tau} = \frac{\partial}{\partial r}\left(k_c \frac{\partial t_c}{\partial r}\right) \quad , r = R_{ci} < r < R_{co}, \tau > 0 \tag{A.44}$$

with the boundary conditions:

$$\begin{aligned} k_c \frac{\partial t_c}{\partial r} &= \tfrac{k_{gp}}{\delta}\left[t_c(R_{ci}) - t_f(R_f)\right] \quad , r = R_{ci}, \quad \text{for all } \tau \\ -k_c \frac{\partial t_c}{\partial r} &= \overline{h}_c\left[t_c(R_{co}) - t_{fl}\right] \qquad , r = R_{co} \quad \text{for all } \tau \end{aligned} \tag{A.45}$$

Following correlations are implemented:

volumetric heat capacity of the fuel

$$(\rho c)_f = c_1 + c_2 t_f + c_3 t_f^2 + c_4 t_f^3 + c_5 t_f^4 \tag{A.46}$$

volumetric heat capacity of the cladding

$$(\rho c)_c = c_7 \tag{A.47}$$

thermal conductivity for the fuel

$$k_f = \frac{c_8}{1 + c_9 \cdot t_f} \tag{A.48}$$

thermal conductivity for the cladding

$$k_c = c_{10} \tag{A.49}$$

thermal conductance of the gas gap

$$\frac{k_{gp}}{\delta} = \min\left\{c_{11} + c_{12} \cdot \overline{t}_f + c_{13} \cdot \overline{t}_f^2, c_{14}\right\} \tag{A.50}$$

$$\text{with} \quad \overline{t}_f = \frac{1}{M_f}\sum_{i=1}^{M_f} t_{f,i} \tag{A.51}$$

convective heat transfer for forced convection (Dittus Boelter)

$$\overline{h}_{c,\,forced\ convection} = \frac{k_l}{d_h} N_{Nu} \tag{A.52}$$

convective heat transfer for nucleate boiling (Jens-Lotte)

$$\overline{h}_{c,nucleate\ boiling} = \frac{q''_{NB}}{t_W - t_{sat}} \tag{A.53}$$

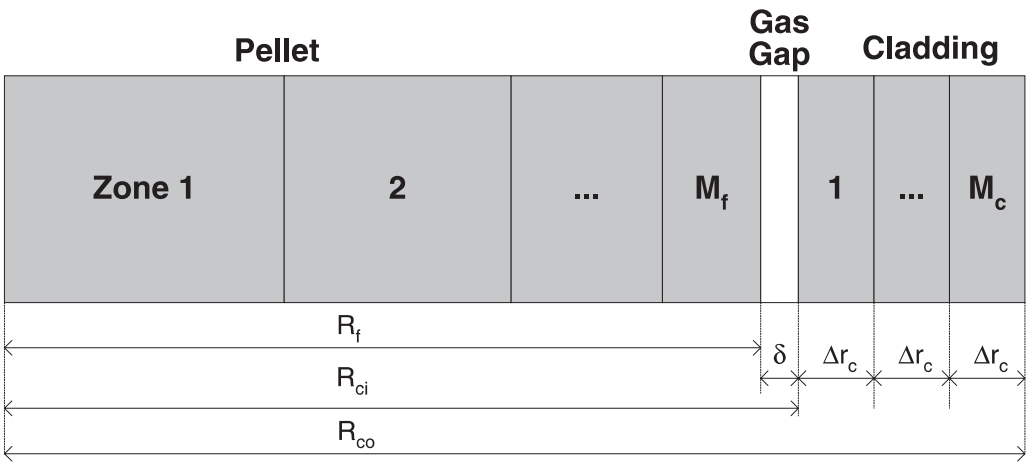

Figure A.1: Nodalization Scheme for the Heat Conduction in the Fuel Rod

A.2.2 Discretization

The fuel pin is radially divided into M_f fuel zones, a gas gap and M_c cladding zones. Fuel zones have the same volume, cladding zones the same thickness.

After long calculations (done explicitly in [114]) one derives

Pellet:

$$\frac{d\bar{t}_{f,1}}{d\tau} = \frac{4M_f}{R_f^2 (\rho c)_f} k_f (t_{f,2}) \frac{\bar{t}_{f,2} - \bar{t}_{f,1}}{\sqrt{2}} + \frac{\bar{q}_f'''}{(\rho c)_f} \tag{A.54}$$

$$\frac{d\bar{t}_{f,i}}{d\tau} = \frac{4M_f}{R_f^2 (\rho c)_f} \left[k_f(t_{f,i}) \frac{\bar{t}_{f,i-1} - \bar{t}_{f,i}}{\sqrt{\frac{i}{i-1}} - \sqrt{\frac{i-2}{i-1}}} - k_f(t_{f,i+1}) \frac{\bar{t}_{f,i} - \bar{t}_{f,i+1}}{\sqrt{\frac{i+1}{i}} - \sqrt{\frac{i-1}{i}}} \right] + \frac{\bar{q}_f'''}{(\rho c)_f} \tag{A.55}$$

$$i = 2, \ldots, M_f - 1$$

$$\frac{d\bar{t}_{f,M_f}}{d\tau} = \frac{4M_f}{R_f^2 (\rho c)_f} \left[k_f(t_{f,M_f}) \frac{\bar{t}_{f,M_f-1} - \bar{t}_{f,M_f}}{\sqrt{\frac{M_f}{M_f-1}} - \sqrt{\frac{M_f-2}{M_f-1}}} - \frac{R_f (\bar{t}_{f,M_f} - \bar{t}_{c,1})}{\frac{R_f (1 - \sqrt{1 - \frac{1}{M_f}})}{k_f(t_f(R_f))} + \frac{2\delta}{k_{gp}} + \frac{\Delta r_c}{k_c}} \right] + \frac{\bar{q}_f'''}{(\rho c)_f} \tag{A.56}$$

with the pellet surface temperature

$$t_f(R_f) = \frac{\frac{R_f\left(1-\sqrt{1-\frac{1}{M_f}}\right)}{k_f(t_f(R_f))}\left(\bar{t}_{c,1}-\bar{t}_{f,M_f}\right)}{\frac{R_f\left(1-\sqrt{1-\frac{1}{M_f}}\right)}{k_f(t_f(R_f))}+\frac{2\delta}{k_{gp}}+\frac{\Delta r_c}{k_c}}+\bar{t}_{f,M_f} \tag{A.57}$$

Cladding:

$$\frac{dt_{c,1}}{d\tau} = k_c\frac{\bar{t}_{c,2}-\bar{t}_{c,1}}{(\rho c)_c(\Delta r_c)^2}+\frac{\frac{\bar{t}_{f,M_f}-\bar{t}_{c,1}}{(\rho c)_c\Delta r_c}}{\frac{R_f\left(1-\sqrt{1-\frac{1}{M_f}}\right)}{k_f(t_f(R_f))}+\frac{\delta}{k_{gp}}+\frac{\Delta r_c}{2k_c}} \tag{A.58}$$

$$\frac{d\bar{t}_{c,j}}{d\tau} = k_c\frac{\bar{t}_{c,j+1}-2\bar{t}_{c,j}+\bar{t}_{c,j-1}}{(\Delta r_c)^2(\rho c)_c} \tag{A.59}$$

$$j = 2,\ldots,M_c-1$$

$$\frac{d\bar{t}_{c,M_c}}{d\tau} = -\frac{\bar{h}_c(t_w-t_{fl})}{(\rho c)_c\Delta r_c}-k_c\frac{\bar{t}_{c,M_c}-\bar{t}_{c,M_c-1}}{(\rho c)_c(\Delta r_c)^2} \tag{A.60}$$

A.2.3 Linearization

The effort to linearize equations A.54-A.56, A.58 -A.60 analytically is not worth the benefit in time. Therefore the equations are linearized numerically with respect to $t_{f,i}, t_{c,i}, q'''$ and the system pressure P. However, these equations are much more detailed than effectively necessary. They are part of the legacy of RAMONA. A simpler set of equations as used in other codes as NUFREQ [79] could be solved analytically and would tidy up this part of MATSTAB. Even though the six differential equations for the fuel contribute quite a large number of equations the system matrix $\mathbf{A}_s$, they do not lead to any numerical difficulties because of their weak spatial coupling.

The implemented equations read as follows.

$$\Delta t_{f,i} = \sum_{j=1}^{M_f}\frac{\partial t_{f,i}}{\partial t_{f,j}}\Delta t_{f,j}+\sum_{j=1}^{M_c}\frac{\partial t_{f,i}}{\partial t_{c,j}}\Delta t_{c,j}+\frac{\partial t_{f,i}}{\partial \bar{q}'''_f}\Delta\bar{q}'''_f+\frac{\partial t_{f,i}}{\partial P}\Delta P \tag{A.61}$$

$$\Delta t_{c,i} = \sum_{j=1}^{M_f}\frac{\partial t_{c,i}}{\partial t_{f,j}}\Delta t_{f,j}+\sum_{j=1}^{M_c}\frac{\partial t_{c,i}}{\partial t_{c,j}}\Delta t_{c,j}+\frac{\partial t_{c,i}}{\partial \bar{q}'''_f}\Delta\bar{q}'''_f+\frac{\partial t_{c,i}}{\partial P}\Delta P \tag{A.62}$$

A.3 Modeling of Thermal-Hydraulics

The thermal-hydraulic model of MATSTAB (RAMONA) is a

- four-equation
- non-homogeneous
- non-equilibrium
- one-dimensional
- two-phase flow

model with constitutive equations for thermodynamic state variables. Thermal non-equilibrium between the phases is accounted for by allowing the liquid in a two-phase mixture to depart from saturated conditions, while the vapor is assumed to be at saturation. Hydrodynamic non-equilibrium, i.e. un-equal velocities of the two phases, is introduced via a slip correlation.

The following assumptions are made

- MATSTAB describes the coolant flows in the pressure vessel, using a single recirculation loop and a single steam line representative for all steam lines and recirculation loops respectively.
- The models allow for the liquid phase to be sub-cooled or saturated, but they restrict the vapor to saturation conditions.
- The flow parameters are assumed to be uniform over a cross section
- Averages of products are set equal to products of averages
- The spatial variation of pressure P is ignored for all thermo-physical property calculations and in the mass and energy balances, but in the momentum balance the axial pressure variation is accounted for.
- Flow channels in the core, downcomer and recirculation loop are of constant cross-section A_c.

Thermodynamic variables are determined at the saturated state corresponding to the system pressure (except the properties of sub-cooled water), and they are calculated as rational functions of pressure A.71 through A.80. The compressibility and thermal expansion of the liquid are approximated by that of saturated liquid. The following description of the TH-model is very brief, because no major changes to the RAMONA model are introduced. The interested user may consult [114] for a complete derivation.

A.3.1 Governing Equations for the Thermal-Hydraulics

The thermal-hydraulic models in MATSTAB are based on the following four conservation equations [45] for mixture momentum, vapor mass, liquid mass and mixture energy.

Mixture momentum balance

The one-dimensional, area-averaged mixture momentum balance is

$$\frac{\partial G_m}{\partial \tau} + \frac{\partial}{\partial z}\left[\alpha \rho_g w_g^2 + (1-\alpha)\rho_l w_l^2\right] = -\frac{\partial P}{\partial z} - g_z \rho_m - f_l \Phi_l^2 \frac{G_m |G_m|}{2\rho_l d_h} \tag{A.63}$$

where the mixture mass flux G_m in the axial direction is

$$G_m = \langle \alpha \rho_g w_g + (1-\alpha)\rho_l w_l \rangle \tag{A.64}$$

The symbols f_l, Φ_l^2 and d_h designate the single-phase Darcy friction factor, computed as if the mixture were flowing as a liquid, the two phase flow friction multiplier and the hydraulic diameter of the channel, wetted by the fluid. The symbol g_z is the gravitational acceleration component in the negative z-direction.

Phasic mass balances for saturated vapor and liquid

The phasic mass balances

$$\frac{\partial}{\partial \tau}(\alpha \rho_g) + \nabla(\rho_g j_g) = \Gamma_V \tag{A.65}$$

$$\frac{\partial}{\partial \tau}[(1-\alpha)\rho_l] + \nabla(\rho_l j_l) = -\Gamma_V \tag{A.66}$$

are used in the form of the mixture volumetric flux divergence.

$$\begin{aligned} \nabla j_m &= \nabla j_g + \nabla j_l = \nabla(\alpha w_g) + \nabla((1-\alpha) w_l) \\ &= \frac{\rho_l - \rho_g}{\rho_l \rho_g}\Gamma_V - \left[\frac{\alpha}{\rho_g}\frac{D_g \rho_g}{D\tau} + \frac{1-\alpha}{\rho_l}\frac{D_l \rho_l}{D\tau}\right] \end{aligned} \tag{A.67}$$

where $\frac{D_k}{D_\tau}$ is the substantial derivative $\frac{\partial}{\partial \tau} + w_k \frac{\partial}{\partial z}$, k = l,g

Mixture energy conservation

$$\frac{\partial}{\partial \tau}[\alpha \rho_g u_g + (1-\alpha)\rho_l u_l] + \frac{\partial}{\partial z}[\alpha \rho_g h_g w_g + (1-\alpha)\rho_l h_l w_l] = \frac{q'_w}{A} + (1-\alpha) q'''_l \tag{A.68}$$

A.3.2 Differential Equations

Pressure

As stated in the assumptions above, local pressure differences and acoustical effects are disregarded. A single system pressure P_{syst} is defined

$$\langle \mathrm{P} \rangle_{\mathrm{syst}} = \frac{1}{\mathrm{V}_1 + \mathrm{V}_2} \int_{\mathrm{V}_1+\mathrm{V}_2} \mathrm{P}\, \mathrm{dV} \tag{A.69}$$

as the pressure, averaged over the volume V_1 of liquid and the volume V_2 of two phase mixture and pure vapor, as shown in figure A.2.

The time rate of change of $\langle P \rangle_{syst}$ is computed by integrating the liquid part of A.67 over V_1 and the two phase part of A.67 over V_2. In the resultant equations, one replaces the volume integrals of ∇j_m by surface integrals and recognizes the continuity of the volumetric flux j at all locations of flow discontinuity and at moving interfaces. By adding up the two equations and solving for the time-derivative $\mathrm{d}\frac{\langle P \rangle_{syst}}{d\tau}$, one reaches after tedious calculations, done explicitly in [114] pages 125ff.

$$\frac{d\,\langle P \rangle_{syst}}{d\tau} = \frac{(Aj)_{FW} + (Aj)_{SL} + \int\limits_{V_2} \frac{\rho_l - \rho_g}{\rho_l \rho_g} \Gamma_V dV}{\int\limits_{V_1+V_2} \left[\alpha \frac{\rho'_g}{\rho_g} + (1-\alpha) \frac{\rho'_l}{\rho_l} \right]} \tag{A.70}$$

where $\rho'_l = \frac{\partial}{\partial P}\rho_l$ and $(Aj)_{FW}$ is the contribution to pressure rise from the feed-water injection. $(Aj)_{SL}$ is the vapor volumetric flow rate entering the steam line, tending thereby to reduce the pressure change rate. The last term accounts for the effects of phase change.

The thermal properties of the coolant $t_{sat}, \rho_f, \rho_l, \rho_g, \rho_m, h_{fg}, c_{p,l}, u_g, u_l, h_g$ and h_l are fitted as functions in $\langle P \rangle_{syst}$.

$$t_{sat}(\mathrm{P}) = \sum_{i=0}^{i=5} a_i \mathrm{P}^{\mathrm{i}} \Big/ \sum_{\mathrm{i}=0}^{\mathrm{i}=5} \mathrm{b_i P^i} \tag{A.71}$$

$$\rho_f(\mathrm{P}) = \sum_{i=0}^{i=4} a_i t_{sat}^{i} \Big/ \sum^{i=3} \qquad sat$$

t

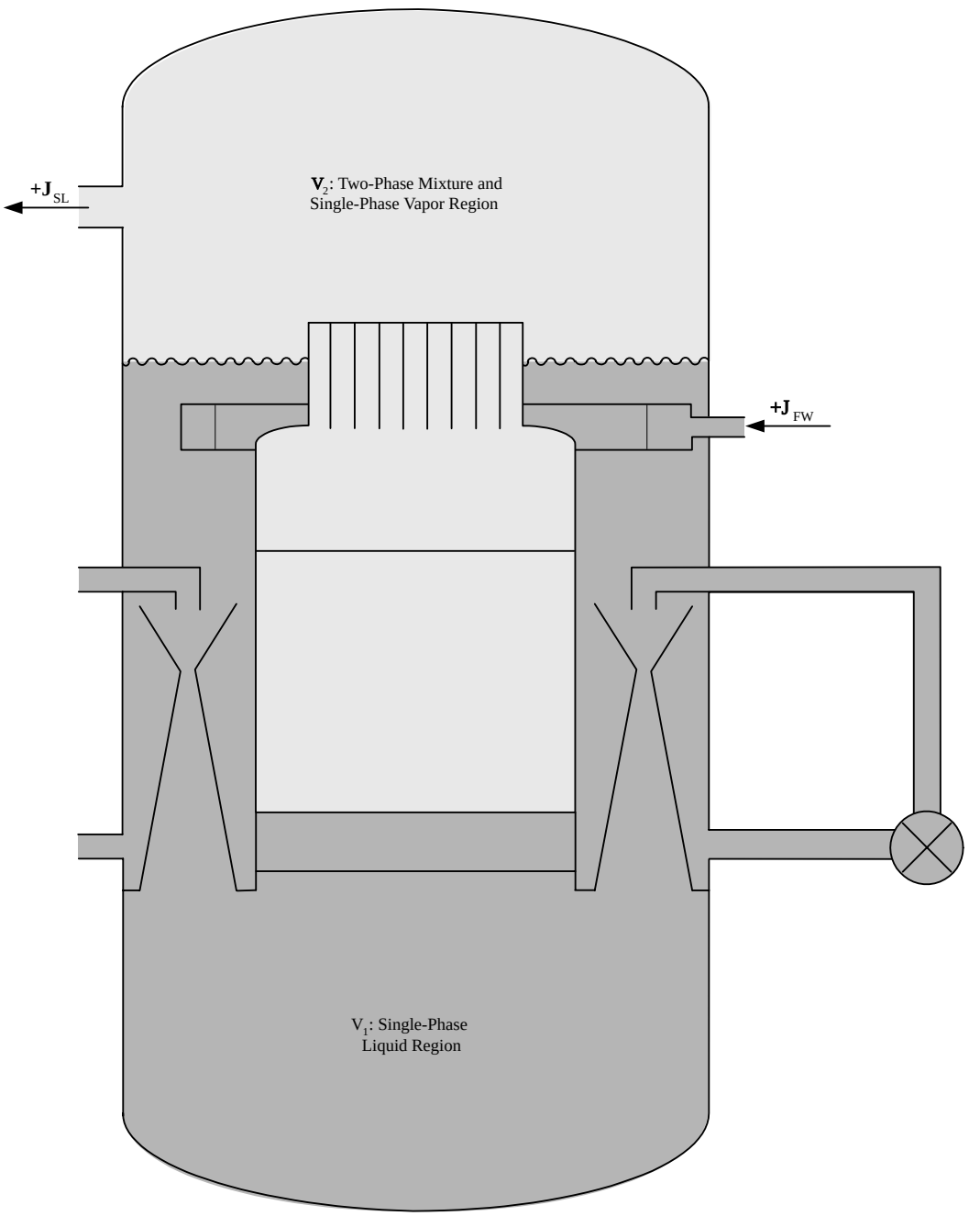

Figure A.2: Integration Regions for System Pressure

$$c_{p,l}(\mathrm{P}) = \sum_{i=0}^{i=4} a_i t_{sat}^i \Big/ \sum_{i=0}^{i=3} b_i t_{sat}^i \tag{A.77}$$

$$u_g(\mathrm{P}) = h_{fg} + \mathrm{P}(1/\rho_\mathrm{f} - 1/\rho_\mathrm{g}) + \mathrm{c_{p,l}}(\mathrm{t_{sat}} - \mathrm{t_{sat}^0}) \tag{A.78}$$

$$u_l(\mathrm{P}) = c_{p,l}(t_l - t_{sat}^0)h_g \qquad = u_g + \mathrm{P}/\rho_\mathrm{g} \tag{A.79}$$

$$h_l = u_l + \mathrm{P}/\rho_\mathrm{l} \tag{A.80}$$

As a result one can eliminate the implicit pressure dependence stemming from the properties in the momentum balance A.63 and decouple it form the mass and energy balances.

Closed-Contour Momentum Balance

To obtain the closed contour momentum balance for a typical contour $\zeta_1$in figure 3.3 on page 27 through the j-th core flow channel, MATSTAB divides the contour into N_s straight segments of constant flow cross section A_i and length L_i. We denote the segment average of the ith segment by

$$< \cdot >_i = \frac{1}{\mathrm{L_i}} \int_0^{\mathrm{L_i}} \cdot \, dz \tag{A.81}$$

A typical segment is shown in figure A.3

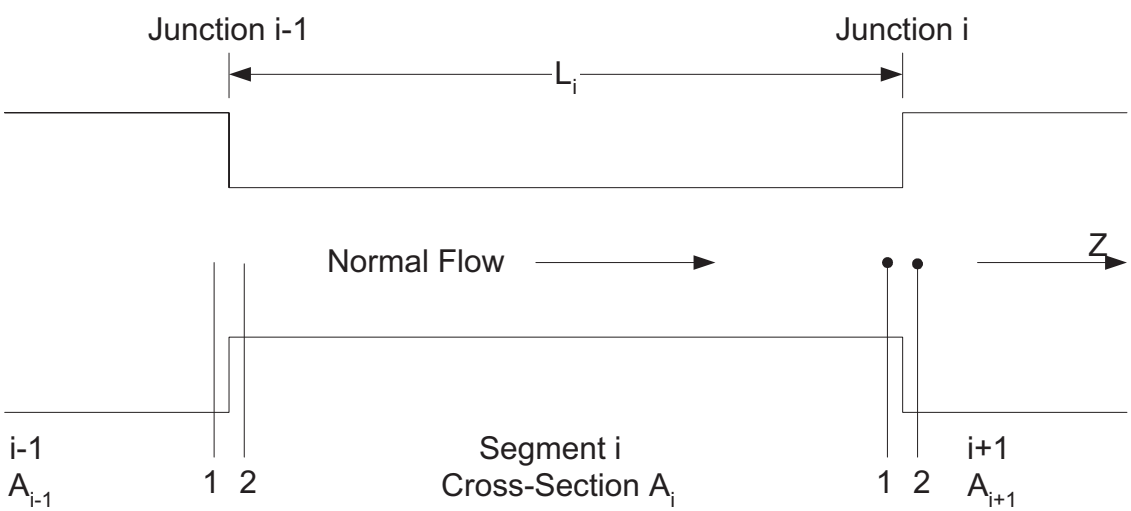

Figure A.3: Notations for Contour Integration of the Momentum Balance

By integrating the momentum balance equation A.63 separately for each one of the N_s segments in the jth contour through the jth core channel, one obtains N_s segment-averaged momentum balances.

$$L_i \frac{d < G_m >_i}{d\tau} = \left\{ P + \left[\alpha \rho_g w_g^2 + (1-\alpha) \rho_l w_l^2 \right] \right\}_{i-1,2} - \left\{ P + \left[\alpha \rho_g w_g^2 + (1-\alpha) \rho_l w_l^2 \right] \right\}_{i,1} - g_{z,i} L_i < \rho_m >_i - \frac{1}{2 d_{h,i}} \int_0^{L_i} \frac{f_l \Phi_l^2}{\rho_l} G_m |G_m| dz \tag{A.82}$$

Next, one adds up the N_s equations for the jth flow contour to obtain a single, ordinary differential equation for the time rate of change of momentum along the closed contour with index j.

$$\frac{d}{d\tau} M_j \equiv \frac{d}{d\tau} \sum_{i=1}^{N_s} L_i \langle G_m \rangle = \sum_{i=1}^{N_s} \Delta \{ P + w_g G_g + w_l G_l \}_j - \left\{ \sum_{i=1}^{N_s} g_{z,i} \langle \rho_m \rangle_i L_i + \frac{1}{2} \sum_{i=1}^{N_s} + \frac{1}{d_{h,i}} \int_0^{L_i} \frac{f_l \Phi_l^2}{\rho_l} G_m |G_m| dz \right\}_j \tag{A.83}$$

The pressure differences across the junction with index i (Figure. A.3) are eliminated with the aid of the jump condition given by

$$P_{i,1} + \frac{1}{2} [G_l w_l + G_g w_g]_1 = P_{i,2} + \frac{1}{2} [G_l w_l + G_g w_g]_2 + \xi_{12} \frac{1}{2} [G_l w_l + G_g w_g]_{A_{min}} \tag{A.84}$$

and therefore

$$\{ P + w_g G_g + w_l G_l \}_j = \frac{1}{2} \{ [w_g G_g + w_l G_l]_2 - [w_g G_g + w_l G_l]_1 - \xi_{12} [w_g G_g + w_l G_l]_{A_m in} \}_j \tag{A.85}$$

A.85 applies to all junctions, except across the mixing throat in the jet pump designated by i=JT, there

$$\Delta \{ P + w_l G_l \}_{JT} = \Delta P_{JT} \tag{A.86}$$

A.83 can now be written as

$$\frac{d M_j}{d\tau} = \Delta P_{JT} - \sum_{i=1}^{N_s} \left\{ g_{z,i} \langle \rho_m \rangle L_i + \frac{1}{2 d_{h,i}} \int_0^{L_i} \frac{f_l \Phi_l^2}{\rho_l} G_m |G_m| dz \right\}_j + \frac{1}{2} \sum_{\substack{i=1 \\ i \neq JT}}^{N_s} \left\{ [w_g G_g + w_l G_l]_2 - [w_g G_g + w_l G_l]_1 \left[1 + \left(\frac{A_1}{A_{min}} \right)^2 \xi_{12} \right] \right\}_j \tag{A.87}$$

The four summands are the pump head, the gravitational head, the frictional pressure loss and the sum of the singular pressure losses (area changes, spacers) along the path.

Mixture Energy

Integrating A.68 over the cell volume V_k and introducing

$$u_m \rho_m = (1-\alpha)\,\rho_l u_l + \alpha \rho_g u_g \tag{A.88}$$

leads to

$$\begin{aligned} \frac{d\,\langle u_m \rho_m \rangle_k}{d\tau} &= (h_g W_g + h_l W_l)_{k-1} - (h_g W_g + h_l W_l)_k \\ &\quad + \left[\langle q'_w \rangle_k + \langle A(1-\alpha)\, q'''_l \rangle_k\right] \frac{V_k}{A_k} \end{aligned} \tag{A.89}$$

Steam Mass

By integrating A.65 over the k-th computational cell, assuming a uniform vapor density and using the divergence theorem one obtains

$$\frac{d\,(m_g)_k}{d\tau} = \langle \Gamma_V \rangle_k \Delta V + (W_g)_{k-1} - (W_g)_k \tag{A.90}$$

A.3.3 Algebraic Equations

Mixture Volumetric Flow

The integral of A.67 over the coolant volume in the vessel yields

$$A_j(z)\, j_{m,j}(z) = A\left(z^+_{core\ inlet}\right) j_{m,j}\left(z^+_{core\ inlet}\right) + \Phi_j(z) \tag{A.91}$$

with

$$z^+_{core\ inlet} = \lim_{\varepsilon \to 0} (z_{core\ inlet} + \varepsilon) \tag{A.92}$$

and the volume expansion

$$\Phi_j(z) = \int_{z_{core\ inlet}}^{z} A_j \left[\frac{\rho_l - \rho_g}{\rho_l \rho_g}\Gamma_V - \frac{\alpha}{\rho_g}\frac{D_g \rho_g}{D_\tau} - \frac{(1-\alpha)}{\rho_l}\frac{D_l \rho_l}{D_\tau}\right]_j dz \tag{A.93}$$

and in the finite difference approximation

$$\Phi_j = V_j \Gamma_v \frac{\rho_l - \rho_g}{\rho_l \rho_g} + W_{g,k-1}\left(\frac{1}{\rho_{g,k}} - \frac{1}{\rho_{g,k-1}}\right) + W_{l,k-1}\left(\frac{1}{\rho_{l,k}} - \frac{1}{\rho_{l,k-1}}\right) \tag{A.94}$$

Slip

MATSTAB treats non-homogeneous two-phase flow, i.e. unequal velocities of the phases with a slip correlation.

$$w_g = \mathrm{Sw_l} + \mathrm{w^0} \tag{A.95}$$

This relates the vapor velocity w_g with the liquid velocity w_l, using the Bankoff-Malnes correlation.

$$\begin{array}{lll} S & = \frac{1-\alpha}{c_1-\alpha} & \alpha \le c_1 - c_{cut} \\ S & = c_2 - c_3(\alpha - c_4) & c_{max} > \alpha > c_1 - c_{cut} \\ S & = c_{\max} & \alpha \ge c_{max} \end{array} \tag{A.96}$$

with the vapor void fraction

$$\alpha = \frac{m_g}{\rho_g \left(\langle P \rangle_{syst} \right) \Delta V} \tag{A.97}$$

Phasic Velocity

From A.67 and A.95 one derives the phasic velocities

$$w_g = \frac{S j_m + (1-\alpha) w^0}{1 + \alpha (S-1)} \tag{A.98}$$

$$w_l = \frac{j_m - \alpha w^0}{1 + \alpha (S-1)} \tag{A.99}$$

Mass Flow Rate

$$W_g = A \rho_g \alpha_g w_g \tag{A.100}$$

$$W_l = A (1-\alpha) \rho_l w_l \tag{A.101}$$

Vapor Generation Rate

The vapor generation rate is computed in two parts

$$\Gamma_V = \Gamma_W + \Gamma_{ph} \tag{A.102}$$

The first part accounts for evaporation due to heat transfer from the wall to the liquid phase. The second part accounts for mass transfer (evaporation or condensation) due to heat transfer between the phases.

$$\Gamma_W = \frac{q'_W/A}{h_{fg} + c_{p,l}\left[(t_{sat} - t_l)\frac{\rho_l}{\rho_g} + \frac{1}{2}(t_w - t_{sat})\left(\frac{\rho_l}{\rho_g} - 1\right)\right]} \tag{A.103}$$

The three terms in the denominator correspond to the heat of evaporation, necessary heating of sub-cooled liquid and removal of energy by the liquid which is returned from the boundary layer to the bulk of liquid.

$$\Gamma_{ph} = \frac{c_1 + c_2\alpha(1-\alpha)}{h_{fg}}\left[(t_l - t_{sat}) + c_3|t_l - t_{sat}|\right] \tag{A.104}$$

The three state variables q'_w, t_l and t_w introduced in A.103 are given in their final form. A detailed derivation can again be found in [114]

Linear Heat Generation Rate:

$$q'_W = \left(\xi\bar{h_c}\right)\left(t_w - t_{fl}\right) - \left(\xi\bar{U}\right)_{lb}\left(t_{fl} - t_{lb}\right) \tag{A.105}$$

where ξ is the heated perimeter. The second term in A.105 accounts for the bypass.

Liquid Temperature:

$$t_l = t_{sat} + \frac{\rho_m u_m - \alpha\rho_g u_g}{(1-\alpha)\rho_l c_{p,l}} \tag{A.106}$$

Equation A.106 is an implicit definition of the liquid temperature because ρ_l and u_g dependent themselves on t_l.

Wall Temperature:

$$t_w = t_c(R_{co}) = t_{fl} + \frac{t_{c,MC} - t_{fl}}{1 + \frac{h_c \Delta r_c}{2k_c}} \tag{A.107}$$

A.3.4 Linearization

Pressure

The linearization of the system pressure A.70 becomes

$$\begin{aligned}\Delta\langle \mathrm{P}\rangle_{\mathrm{syst}} &= \frac{\partial\langle \mathrm{P}\rangle_{\mathrm{syst}}}{\partial \mathrm{P}}\Delta\langle \mathrm{P}\rangle_{\mathrm{syst}} + \frac{\partial\langle \mathrm{P}\rangle_{\mathrm{syst}}}{\partial \Gamma_{\mathrm{v}}}\Delta\Gamma_{\mathrm{v}} + \frac{\partial\langle \mathrm{P}\rangle_{\mathrm{syst}}}{\partial \mathrm{t_l}}\Delta \mathrm{t_l} \\ &= \frac{\partial\langle \mathrm{P}\rangle_{\mathrm{syst}}}{\partial \mathrm{P}}\Delta\langle \mathrm{P}\rangle_{\mathrm{syst}} + \frac{\frac{\rho_{\mathrm{l}}-\rho_{\mathrm{g}}}{\rho_{\mathrm{l}}\rho_{\mathrm{g}}\mathrm{V_{k_1}}}}{\alpha\frac{\rho'_{\mathrm{g}}}{\rho_{\mathrm{g}}} + (1-\alpha)\frac{\rho'_{\mathrm{l}}}{\rho_{\mathrm{l}}}\mathrm{V_{k_{1,2}}}}\Delta\Gamma_{\mathrm{v}} \\ &+ \frac{\Gamma_v V_{k_1}}{\rho_g}\left(\frac{\left[\alpha\frac{\rho'_g}{\rho_g}\rho_l + (1-\alpha)\rho'_l\right] - \left(\frac{\rho_l}{\rho_g}-1\right)\alpha\rho'_g}{\left[\alpha\frac{\rho'_g}{\rho_g}\rho_l + (1-\alpha)\rho'_l\right]^2 V_{k_{1,2}}}\right)\frac{\partial\rho_l}{\partial t_l}\Delta t_l\end{aligned} \tag{A.108}$$

The value of $\frac{\partial\langle \mathrm{P}\rangle_{\mathrm{syst}}}{\partial \mathrm{P}}\Delta\langle \mathrm{P}\rangle_{\mathrm{syst}}$ is derived numerically while $\frac{\partial\rho_l}{\partial t_l}$ comes easily from A.73

Momentum Balance

The linearization of the momentum balance A.83 becomes

$$\Delta M = \frac{\partial M}{\partial \mathrm{P}}\Delta \mathrm{P} + \frac{\partial \mathrm{M}}{\partial \alpha}\Delta\alpha + \frac{\partial \mathrm{M}}{\partial \mathrm{t_l}}\Delta \mathrm{t_l} + \frac{\partial \mathrm{M}}{\partial \mathrm{W_l}}\Delta \mathrm{W_l} + \frac{\partial \mathrm{M}}{\partial \mathrm{W_g}}\Delta \mathrm{W_g} \tag{A.109}$$

This linearization is done numerically due to the complexity of A.83.

Mixture Energy

The linearization of the mixture energy A.89 becomes

$$\begin{aligned}\Delta u_m\rho_m &= \frac{\partial u_m\rho_m}{\partial \mathrm{P}}\Delta \mathrm{P} + \frac{\partial \mathrm{u_m}\rho_{\mathrm{m}}}{\partial \mathrm{t_l}}\Delta \mathrm{t_l} + \frac{\partial \mathrm{u_m}\rho_{\mathrm{m}}}{\partial \mathrm{W_{l,k}}}\Delta \mathrm{W_{l,k}} + \frac{\partial \mathrm{u_m}\rho_{\mathrm{m}}}{\partial \mathrm{W_{l,k-1}}}\Delta \mathrm{W_{l,k-1}} \\ &+ \frac{\partial u_m\rho_m}{\partial W_{l,g}}\Delta W_{l,g} + \frac{\partial u_m\rho_m}{\partial W_{l,g-1}}\Delta W_{l,g-1} + \frac{\partial u_m\rho_m}{\partial q'_w}\Delta q'_w + \frac{\partial u_m\rho_m}{\partial q'''_l}\Delta q'''_l + \frac{\partial u_m\rho_m}{\partial \alpha}\Delta\alpha \\ &= -h_{l,k}\Delta W_{l,k} + h_{l,k-1}\Delta W_{l,k-1} - h_{g,k}\Delta W_{g,k} + h_{g,k-1}\Delta W_{g,k-1} \\ &+ \frac{V_k}{A_k}\Delta q'_w + V_k(1-\alpha)\Delta q'_w - V_k q'''_l\Delta\alpha\end{aligned} \tag{A.110}$$

$\frac{\partial u_m\rho_m}{\partial \mathrm{P}}$ and $\frac{\partial u_m\rho_m}{\partial t_l}$ is neglected.

Steam Mass

The linearization of the steam mass A.90 becomes

$$\begin{aligned}\Delta m_{g,k} &= \frac{\partial m_{g,k}}{\partial \Gamma_{v,k}}\Delta\Gamma_{v,k} + \frac{\partial m_{g,k}}{\partial W_{g,k}}\Delta W_{g,k} + \frac{\partial m_{g,k}}{\partial W_{g,k-1}}\Delta W_{g,k-1} \\ &= V_k\Delta\Gamma_v - \Delta W_{g,k} + \Delta W_{g,k-1}\end{aligned} \tag{A.111}$$

Mixture Volumetric Flux

The linearization of the volumetric mixture flux A.67 becomes

$$\begin{aligned}A\Delta j_m &= A(z^+_{coreinlet})\Delta j_m(z^+_{coreinlet}) \\ &\quad + \frac{\partial\Phi}{\partial\Gamma_v}\Delta\Gamma_v + \frac{\partial\Phi}{\partial W_{g,k-1}}\Delta W_{g,k-1} + \frac{\partial\Phi}{\partial W_{l,k-1}}\Delta W_{l,k-1} \\ &= V_k\frac{\rho_l-\rho_g}{\rho_l\rho_g}\Delta\Gamma_v + \left(\frac{1}{\rho_{l,k}} - \frac{1}{\rho_{l,k-1}}\right)\Delta W_{l,k-1} + \left(\frac{1}{\rho_{g,k}} - \frac{1}{\rho_{g,k-1}}\right)\Delta W_{g,k-1}\end{aligned} \tag{A.112}$$

$\frac{\partial\Phi}{\partial P}$ and $\frac{\partial\Phi}{\partial t_l}$ is neglected.

Slip

The linearization of the slip A.96 becomes

$$\begin{aligned}\Delta S &= \tfrac{\partial S}{\partial\alpha}\Delta\alpha \\ &= \tfrac{1-c_1}{(c_1-\alpha)^2}\Delta\alpha \quad && \alpha \le c_1 - c_{cut} \\ &= -c_3\Delta\alpha \quad && c_{max} > \alpha > c_1 - c_{cut} \\ &= 0 \quad && \alpha \ge c_{max}\end{aligned} \tag{A.113}$$

Phasic Velocity

The linearization of the gas velocity A.98 becomes

$$\begin{aligned}\Delta w_g &= \frac{\partial w_g}{\partial\alpha}\Delta\alpha + \frac{\partial w_g}{\partial j_m}\Delta j_m + \frac{\partial w_g}{\partial S}\Delta S \\ &= \frac{w_g(1-S)-w^0}{1+\alpha(S-1)}\Delta\alpha + \frac{S}{1+\alpha(S-1)}\Delta j_m + \frac{j_m - w_g\alpha}{1+\alpha(S-1)}\Delta S\end{aligned} \tag{A.114}$$

Mass Flow Rate

The linearization of the liquid mass flow rate A.101 becomes

$$\begin{aligned}\Delta W_l &= \frac{\partial W_l}{\partial \mathrm{P}}\Delta \mathrm{P} + \frac{\partial \mathrm{W_l}}{\partial \alpha}\Delta\alpha + \frac{\partial \mathrm{W_l}}{\partial \mathrm{S}}\Delta \mathrm{S} + \frac{\partial \mathrm{W_l}}{\partial \mathrm{t_l}}\Delta \mathrm{t_l} + \frac{\partial \mathrm{W_l}}{\partial \mathrm{j_m}}\Delta \mathrm{j_m} \\ &= A(1-\alpha)w_l\frac{\partial \rho_l}{\partial \mathrm{P}}\Delta \mathrm{P} \\ &\quad - \rho_l A\frac{-[1+\alpha(S-1)]w^0 - (j_m - \alpha w^0)(S-1)}{[1+\alpha(S-1)]^2}\Delta\alpha \\ &\quad - A(1-\alpha)\rho_l\frac{(j_m-\alpha w^0)\alpha}{[1+\alpha(S-1)]^2}\Delta S \\ &\quad + A(1-\alpha)w_l\frac{\partial \rho_l}{\partial t_l}\Delta t_l \\ &\quad + \frac{A(1-\alpha)\rho_l}{1+\alpha(S-1)}\Delta j_m\end{aligned} \tag{A.115}$$

The linearization of the gas mass flow rate A.100 becomes

$$\begin{aligned}\Delta W_g &= \frac{\partial W_g}{\partial \mathrm{P}}\Delta \mathrm{P} + \frac{\partial \mathrm{W_g}}{\partial \alpha}\Delta\alpha + \frac{\partial \mathrm{W_g}}{\partial \mathrm{w_g}}\Delta \mathrm{w_g} \\ &= A\alpha w_g\frac{\partial \rho_g}{\partial \mathrm{P}}\Delta \mathrm{P} + \mathrm{A}\rho_\mathrm{g}\mathrm{w_g}\Delta\alpha + \mathrm{A}\alpha\rho_\mathrm{g}\Delta \mathrm{w_g}\end{aligned} \tag{A.116}$$

Vapor Generation Rate

The linearization of the vapor generation rate A.102 becomes

$$\Delta\Gamma_v = \frac{\partial \Gamma_v}{\partial \mathrm{P}}\Delta \mathrm{P} + \frac{\partial \Gamma_\mathrm{v}}{\partial \alpha}\Delta\alpha + \frac{\partial \Gamma_\mathrm{v}}{\partial \mathrm{t_l}}\Delta \mathrm{t_l} + \frac{\partial \Gamma_\mathrm{v}}{\partial \mathrm{t_w}}\Delta \mathrm{t_w} + \frac{\partial \Gamma_\mathrm{v}}{\partial \mathrm{q'_w}}\Delta \mathrm{q'_w} \tag{A.117}$$

This linearization is done numerically due to the complexity of A.102.

Linear Heat Generation Rate

The linearization of the linear heat generation rate A.105 becomes

$$\begin{aligned}\Delta q'_w &= \frac{\partial q'_w}{\partial \mathrm{P}}\Delta \mathrm{P} + \frac{\partial \mathrm{q'_w}}{\partial \mathrm{t_w}}\Delta \mathrm{t_w} + \frac{\partial \mathrm{q'_w}}{\partial \mathrm{t_l}}\Delta \mathrm{t_l} \\ &= \frac{\partial q'_w}{\partial \mathrm{P}}\Delta \mathrm{P} + \frac{\partial \mathrm{q'_w}}{\partial \mathrm{W_l}}\Delta \mathrm{W_l} \\ &\quad + (4\xi\bar{h}_{c,boil} + \xi\bar{h}_{c,nonboil})\Delta t_w - \xi\bar{h}_{c,nonboil}\Delta t_l\end{aligned} \tag{A.118}$$

The first term is linearized numerically due to the manyfold dependence on P.

Liquid Temperature

The linearization of the liquid temperature A.106 becomes

$$\Delta t_l = \frac{\partial t_l}{\partial t_{l,0}}\Delta t_{l,0} + \frac{\partial t_l}{\partial \mathrm{P}}\Delta \mathrm{P} + \frac{\partial \mathrm{t_l}}{\partial \alpha}\Delta\alpha + \frac{\partial \mathrm{t_l}}{\partial \mathrm{u_m}\rho_\mathrm{m}}\Delta \mathrm{u_m}\rho_\mathrm{m} \tag{A.119}$$

This linearization is done numerically for all parts. The work of doing this by hand does not correspond to the benefits.

Wall Temperature

The linearization of the wall temperature A.107 becomes

$$\Delta t_w = \frac{\partial t_w}{\partial t_{0,w}}\Delta t_{0,w} + \frac{\partial t_w}{\partial \mathrm{P}}\Delta \mathrm{P} + \frac{\partial \mathrm{t_w}}{\partial \mathrm{t_{c,MC}}}\Delta \mathrm{t_{c,MC}} + \frac{\partial \mathrm{t_w}}{\partial \mathrm{t_l}}\Delta \mathrm{t_l} \tag{A.120}$$

Also this linearization is done numerically for all parts due to the same reasons as above.

A.4 The Numerical Linearization

The implemented numerical scheme to linearize numerically is very simple. The equation is evaluated once for the steady state and once with one parameter slightly disturbed. The linearization of $g(\alpha)$ with respect to α is therefore

$$\Delta g(\alpha) = \frac{g(\alpha + \delta\alpha) - g(\alpha)}{\delta\alpha} \tag{A.121}$$

The size of $\delta\alpha$ is chosen so small, that a small change in $\delta\alpha$ would not change $\Delta g(\alpha)$. Using A.121 is very fast, though not elegant.